Eur. Phys. J. Appl. Phys. **49**, 10401 (2010)
DOI: 10.1051/epjap/2009193

THE EUROPEAN PHYSICAL JOURNAL APPLIED PHYSICS

Regular Article

Dielectric measurements in large frequency and temperature ranges of an aromatic polymer

S. Diaham[1,2,a], M.-L. Locatelli[1,2], T. Lebey[1,2], and S. Dinculescu[1,2]

[1] Université de Toulouse, UPS-INPT, LAPLACE (Laboratoire Plasma et Conversion d'Énergie), 118 route de Narbonne, 31062 Toulouse Cedex 9, France
[2] CNRS, LAPLACE, 31062 Toulouse, France

Received: 3 July 2009 / Received in final form: 10 September 2009 / Accepted: 12 October 2009
Published online: 26 November 2009 –

Abstract. The characterization of the BPDA/PDA polyimide (PI) at high temperature up to 400 °C, thanks to dielectric relaxation spectroscopy (DRS) in the 10^{-1} Hz to 10^{6} Hz frequency range, allows the determination of the dc electrical conductivity (σ_{dc}). In such a high temperature range, the dielectric spectra are modified by the extrinsic electrode polarization phenomenon (EP) response. A model is proposed which coupled to the DRS results allows evidencing and quantifying the effect of the EP. The proposed method gives a simple way to determine the intrinsic σ_{dc} values from the effective ac dielectric response, improving the accuracy and reducing the duration of measurement. For BPDA/PDA PI, the resulting σ_{dc} values range from 4×10^{-11} to 8×10^{-6} $\Omega^{-1}\,m^{-1}$ for temperatures between 200 and 400 °C, with an activation energy of the conduction phenomenon of 0.55 eV.

PACS. 72.20.-i Conductivity phenomena in semiconductors and insulators – 77.22.-d Dielectric properties of solids and liquids – 77.22.Gm Dielectric loss and relaxation

1 Introduction

Polymers are the most used insulating materials in electrical and electronic engineering industries due to their excellent thermal, electrical, and mechanical properties related to an easy processability [1]. The knowledge of their electrical properties appears as very important today due to the currently increasing demand for high temperature power electronic applications (>200 °C) [2–5]. Nevertheless, little is known about the electrical properties of the thermo-stable polymers above 200 °C.

The electrical properties of dielectric materials are usually studied through metal-insulator-metal structures (MIMS), using dc current conduction experiments and dielectric relaxation spectroscopy (DRS) [6–17]. However, although DRS can be a powerful and fast tool for measuring the electrical conductivity of the dielectric materials versus temperature [18–25], very few works are dedicated to this measurement technique above 200 °C [26]. Indeed, dc conductivity can be measured through the Ohmic conduction phenomenon occurring at low frequency and/or at high temperature (LF/HT) [27]. However, the high temperature dielectric spectra of MIMS are often modified by interfacial relaxations such as electrode polarization (EP) due to the relaxation of thin space-charge capacitor layers built up in the vicinity of the bulk-electrode interfaces [28]. So, EP adds an extrinsic component to the intrinsic bulk properties, and makes the quantification of the dc conductivity difficult. The use of physico-analytic models is therefore required to extract the intrinsic electrical properties from the effective dielectric response of MIMS [29–35].

The aim of this paper is to show that DRS can be an efficient technique to determine high temperature dc conductivity when it is coupled to a physico-analytic modeling of the experimental data. As an illustration, dielectric measurements have been performed up to 400 °C on MIMS using a polyimide (PI) inter-electrode insulating layer in an extended frequency range down to 10^{-1} Hz completing our previous work [26].

2 Experimental part

The biphenyltetracarboxylic dianhydride acid *p*-phenylene diamine (BPDA/PDA) polyimide (PI) has a glass transition temperature above 350 °C and appears as one of the more thermo-stable polymers. This material has been chosen here in order to provide an experimental illustration of EP and dc conductivity characterization problem. Dielectric properties have been investigated using MIMS with 2 μm-thick PI films. The material is spin-coated from a viscous solution on a polished and cleaned golden stainless

[a] e-mail: sombel.diaham@laplace.univ-tlse.fr

steel substrate, before being cured at 400 °C for 1 h under a nitrogen atmosphere in order to remove residual solvent and to complete the PI chemical reaction. Gold (Au) circular upper electrodes of 5 mm diameter were evaporated under vacuum onto the PI surface in order to achieve the Au–PI–Au MIMS. The infra-red (FTIR) spectra of PI (not given here) have shown good chemical formation of the imide rings in the macromolecular structure.

The dielectric properties in PI have been investigated by DRS in the frequency and temperature ranges from 10^{-1} to 10^{6} Hz and from 100 to 400 °C, respectively thanks to the capacitance (C_P) and the loss factor ($\tan\delta$) measurements under an ac sinusoidal applied voltage of 500 mV rms [36]. The measurements have been plotted according to the complex permittivity formalism ($\varepsilon^* = \varepsilon' - j\varepsilon''$, where ε' and ε'' are respectively the real and imaginary parts of the complex permittivity). At LF/HT, the dipolar dielectric response has been intensively described by Jonscher in his "universal" response approach and follows the fractional power-law given by [37,38]:

$$\varepsilon'(\omega) \propto \varepsilon''(\omega) \propto \omega^{n-1}, \quad (1)$$

where ω is the pulsation and n is the exponent of the power-law ($0 \leq n \leq 1$).

The so-called ac conductivity σ_{ac} in dielectric materials expressed in the frequency domain may be given by [39]:

$$\sigma_{ac}(\omega) = \omega\varepsilon_0\varepsilon''(\omega), \quad (2)$$

where ε_0 is the vacuum permittivity ($\varepsilon_0 = 8.854 \times 10^{-12}$ F m^{-1}).

Moreover, the dielectric loss factor $\tan\delta(\tan\delta = \varepsilon''/\varepsilon')$ is exploited as well because it allows a shift of the different relaxation peaks towards higher frequencies, which are no longer coupled to the conduction component [35].

These measurements have been performed using both a Novocontrol Alpha-A analyzer ($f = 10^{-1}$ to 4×10^5 Hz, $T = 100$ to 300 °C ± 0.1 °C under N_2 atmosphere) with a ZGS active sample cell and an HP 4194A LCR meter ($f = 10^2$ to 10^6 Hz) coupled with a Signatone S-1060R probe station and a heating chuck system ($T = 300$ to 400 °C ± 1 °C in air). Prior to the measurements, the sample is dried for a few minutes at 100 °C to remove moisture from the PI films. The dielectric properties were recorded with a temperature step of 10 °C with a 5 °C min^{-1} heating slope between two consecutive steps. The results presented in the following sections are independent of the heating or cooling measurement runs.

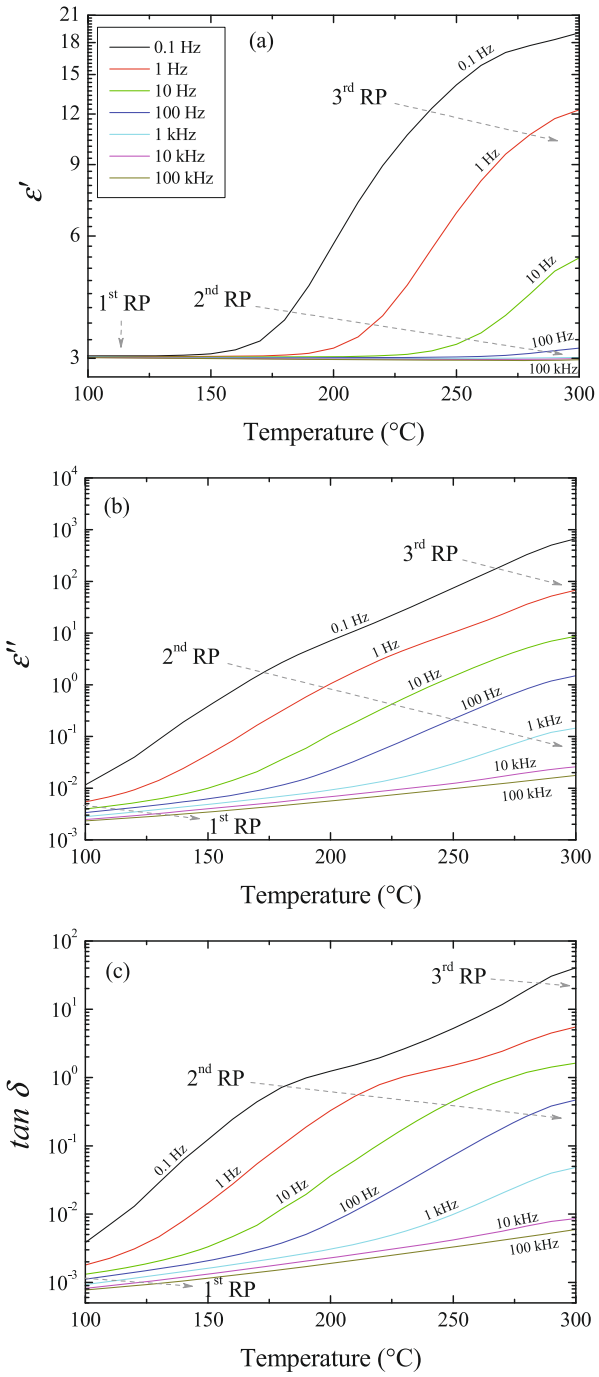

Fig. 1. (Color online) Temperature dependence of (a) the real part ε', (b) imaginary part ε'' of the complex permittivity ε^*, and (c) the loss factor $\tan\delta$ in polyimide MIMS from 100 to 300 °C and for constant frequencies between 10^{-1} and 10^5 Hz.

3 Results and discussion

3.1 DRS temperature and frequency dependences in PI MIMS

Figure 1 shows the dielectric response of PI versus temperature up to 300 °C for different isochronal curves from 10^{-1} to 10^5 Hz. Three relaxation processes (RPs) are observed. The first one (1st RP) appears around 100 °C and shifts toward higher temperature with increasing frequency. It is characterized by both a small change in the dielectric strength $\Delta\varepsilon' < 0.30$ (cf. Fig. 1a) and the occurrence of a dielectric loss peak of low magnitude (cf. Figs. 1b and 1c). It is related to the α-relaxation or MWS process, known to be present in PI below 200 °C, and which corresponds according to the literature to a bulk space-charge relaxation [26,40–42]. When decreasing the

https://doi.org/10.1051/epjap/2009193 Published online by Cambridge University Press

frequency, the α-relaxation shifts towards lower temperatures and the lowest frequency polarization phenomena appear. The two other polarization phenomena (2nd and 3rd RP) also appear through a drop in the real part ε' of the complex permittivity. Indeed, large changes in the dielectric strength $\Delta\varepsilon'$ are observed (up to 19, as shown in Fig. 1a). They are related to two high dielectric losses peaks ($\tan\delta > 1$). Such high values of $\Delta\varepsilon'$ cannot be explained by the PI intrinsic dipolar relaxations. For the latter for instance, the polarization process at a high concentration of dipoles of 10^{22} cm^{-3} whose dipole moments would be of 2 Debyes (which is a huge value) would only induce a permittivity increase about 7 [43]. These two RPs are therefore assumed to be due to electrode polarization (EP) phenomena appearing in MIMS as a result of the motions of mobile charge carriers under the influence of the dc conduction phenomenon.

Figure 2 shows the dielectric spectra of PI MIMS versus frequency where it is possible to observe the frequency changes of the three RPs in the temperature range between 200 and 400 °C. The α-relaxation appears here from 10 kHz to 1 MHz for temperatures between 200 and 320 °C and shifts towards a higher frequency with increasing the temperature. The other two RPs, referred here as the ρ- and the ρ^*-relaxations, corresponding to the EP phenomena appear above 200 °C and over the entire frequency range investigated. Such RPs have never been observed previously by DRS due to the usual temperature range of characterization of PI below 250 °C. Last, the $1/f$ dependence of ε'' and $\tan\delta$ at a low frequency starting from 200 °C and their continuous shift towards higher frequencies with increasing temperature (cf. Figs. 2b and 2c) are observed.

From a theoretical point of view, at low fields and in a broadband frequency and/or a wide temperature range of investigation, several dielectric processes have been identified to govern the dielectric response of polar dielectric materials [44]. Among them, the interfacial processes such as the Maxwell–Wagner–Sillars (MWS) relaxation or the EP mainly control the LF/HT dielectric response. The pure dc conduction being characterized by a plateau (i.e. an invariance) at a low frequency, it is usual to express the relation between the ac conductivity and the dc conductivity as follows [37,38]:

$$\sigma_{ac}(\omega) = \sigma_{dc} + K\omega^n, \tag{3}$$

where σ_{dc} is the dc conductivity, K is a temperature-dependent parameter, and n is the exponent of the power-law (close to 1). The frequency-dependent term corresponds to the different bulk dipolar relaxations that have no influence on σ_{dc} at a low frequency.

Figure 3 shows the frequency dependence of σ_{ac}, for isothermal curves between 100 and 400 °C. σ_{ac} changes linearly versus frequency exhibiting a slope close to unity ($0.98 \leq n \leq 1$), and remains quasi frequency-independent at lower frequencies. Such a behavior demonstrates the thermally activated character of the dc bulk conductivity [21,45]. Last, for temperatures above 200 °C and at a low frequency, a slight decrease in σ_{ac} appears for frequencies below the plateau region. This decrease is probably due to the EP occurrence as a result of the motions of mobile charges over macroscopic distances in PI. The non constant part of the σ_{ac} spectrum at LF/HT shifts towards higher frequencies with increasing the temperature, leading to an increase in the charge carrier mobility. The EP therefore tends to be superimposed on the dc bulk conductivity σ_{dc} [21–24].

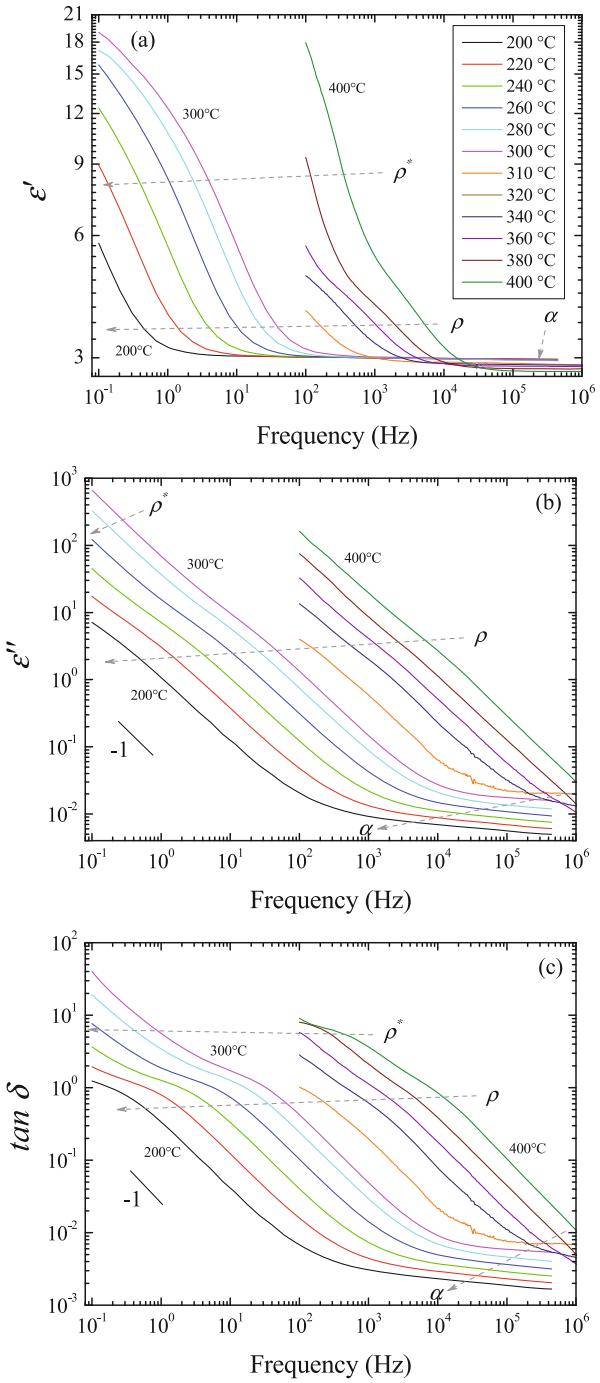

Fig. 2. (Color online) Frequency dependence of (a) the real part ε', (b) imaginary part ε'' of the dielectric complex permittivity ε^*, and (c) the loss factor $\tan\delta$ in polyimide MIMS from 10^{-1} to 10^6 Hz and for constant temperatures between 200 and 400 °C.

https://doi.org/10.1051/epjap/2009193 Published online by Cambridge University Press

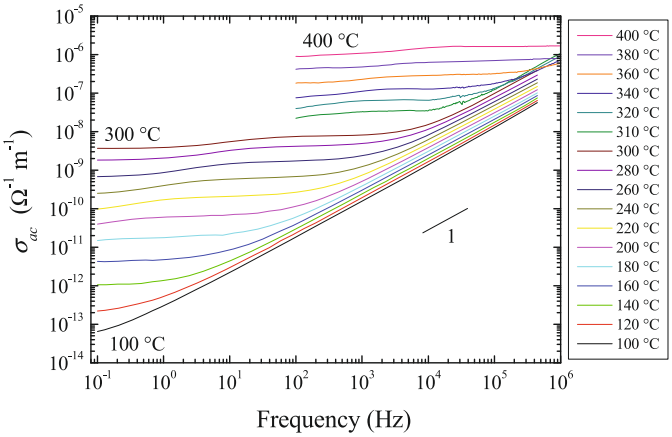

Fig. 3. (Color online) Frequency dependence of the ac conductivity in polyimide MIMS from 10^{-1} to 10^{6} Hz and for constant temperatures between 100 and 400 °C.

3.2 EP behavior and dc conductivity extraction

The different relaxation processes (i.e. dipolar and space-charge) appearing in the dielectric responses can be taken into account using the empirical Havriliak–Negami (H−N) model [46,47], which is a combination of the Cole–Cole symmetric function and of the Cole–Davidson asymmetric one [48,49]. For several relaxation processes, the H−N equation associated with a conduction term is given by [50,51]:

$$\varepsilon^*(\omega) = \varepsilon'_\infty + \sum_{i=1}^{N} \frac{(\Delta\varepsilon')_i}{[1+(j\omega\tau_i)^{\alpha_{HN_i}}]^{\beta_{HN_i}}} - j\left(\frac{\sigma_{dc}}{\varepsilon_0\omega}\right)^s, \quad (4)$$

where $\Delta\varepsilon' = \varepsilon'_S(\omega = 0) - \varepsilon'_\infty(\omega = \infty)$ is the dielectric strength, τ is the mean relaxation time, and $(\alpha_{HN})_i$ and $(\beta_{HN})_i$ are the empirical shape parameters related respectively to the symmetric and asymmetric broadening of the relaxation time distribution function ($0 < (\alpha_{HN})_i \leq 1$ and $0 < (\beta_{HN})_i \leq 1$). The index i represents the different relaxations involved (usually between 1 and 3), and s is the empirical exponent close to unity characterizing the ohmic conduction σ_{dc}. Space charge presents a frequency-dependence close to a near-Debye behavior, qualitatively similar to the dipolar relaxation, allows the description of EP thanks to the H−N function [32,34].

Considering the PI MIMS results given above, equation (4) is used for the data processing where $i = 1, 2$, and 3 represent respectively the α-, ρ-, and ρ^*-relaxations and s is the empirical exponent close to unity for the Ohmic conduction. The fitting procedure consists in a first step of an EP quantification, then the EP is subtracted from the effective dielectric response, and last, the dc conductivity σ_{dc} in PI is quantified accurately in the temperature range investigated. The computing procedure is based on the Levenberg–Marquardt method. Several program runs (of more than hundred iterations for each fitting run) were performed for each procedure, yielding to identical results (i.e. correlation coefficient $0.98 \leq r^2 \leq 1$).

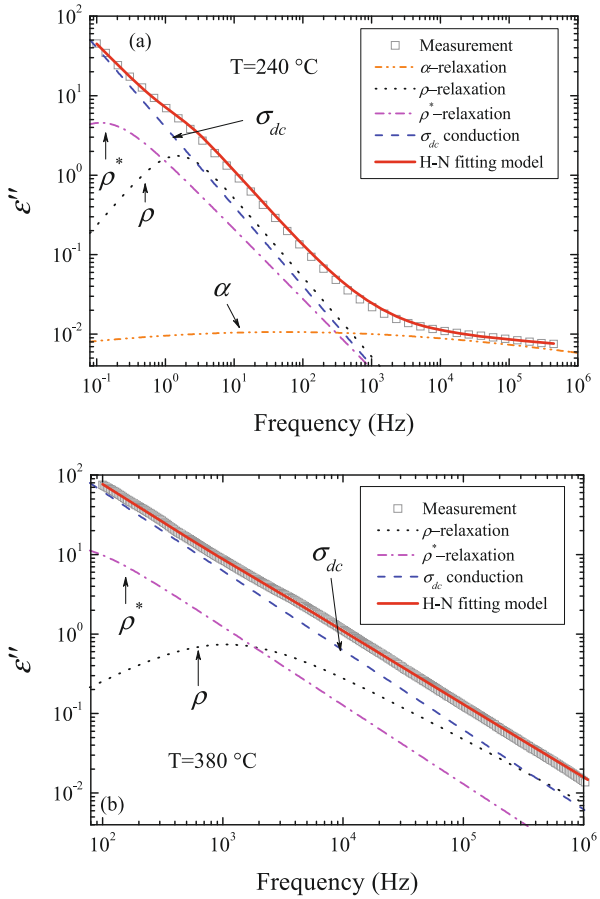

Fig. 4. (Color online) Examples of the fitting procedure performed on the imaginary part ε'' of the complex permittivity ε^* in polyimide MIMS at (a) 240 °C and (b) 380 °C.

Figure 4 presents two examples of the fitting procedure performed simultaneously on both the real and imaginary parts of the complex permittivity for two different temperatures (240 and 380 °C), separating the influence of each of the three relaxation processes and of the conduction phenomenon. From 200 to 300 °C, the dielectric response in PI MIMS is the sum of the α-, the ρ-, the ρ^*-relaxations, and the conduction σ_{dc}, whereas above 300 °C, it is only composed of the ρ-, the ρ^*-relaxations, and σ_{dc}. According to the values of the shape parameters, the α-relaxation exhibits a broad distribution of its relaxation time. Its symmetric shape parameter $(\alpha_{HN})_1$ varies from 0.17 to 0.11 between 200 and 300 °C whereas the asymmetric one $(\beta_{HN})_1$ remains equal to 1. This Cole–Cole behavior is in good agreement with typical changes in the distribution of the relaxation times found in the literature for organic materials [12,52,53]. On the contrary, the $(\alpha_{HN})_2/(\beta_{HN})_2$ and $(\alpha_{HN})_3/(\beta_{HN})_3$ parameters of the respective ρ- and ρ^*-relaxations corresponding to the EP have confirmed the near-Debye behavior (with high values of the shape parameters between 0.81 and 1). Such a result is in close agreement with the typical dielectric behavior of a space charge at the bulk-electrode interfaces of MIMS relaxing with a unique relaxation time.

https://doi.org/10.1051/epjap/2009193 Published online by Cambridge University Press

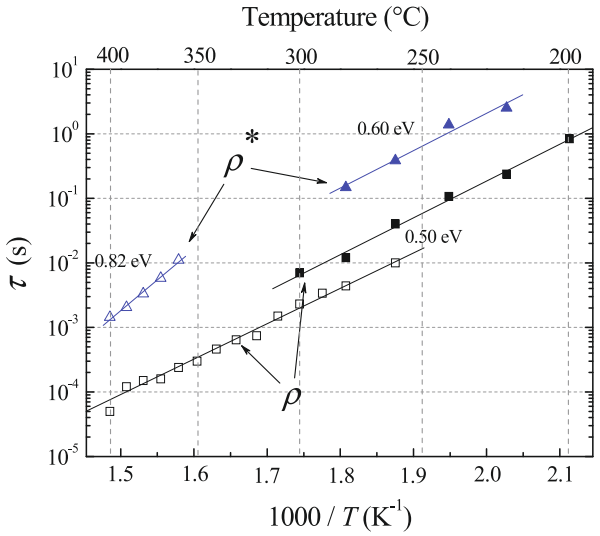

Fig. 5. (Color online) Temperature dependence of the mean relaxation times for both the ρ- and ρ^*-relaxations between 200 and 400 °C. The filled and the open symbols correspond to the Novocontrol and the HP experimental set-up, respectively.

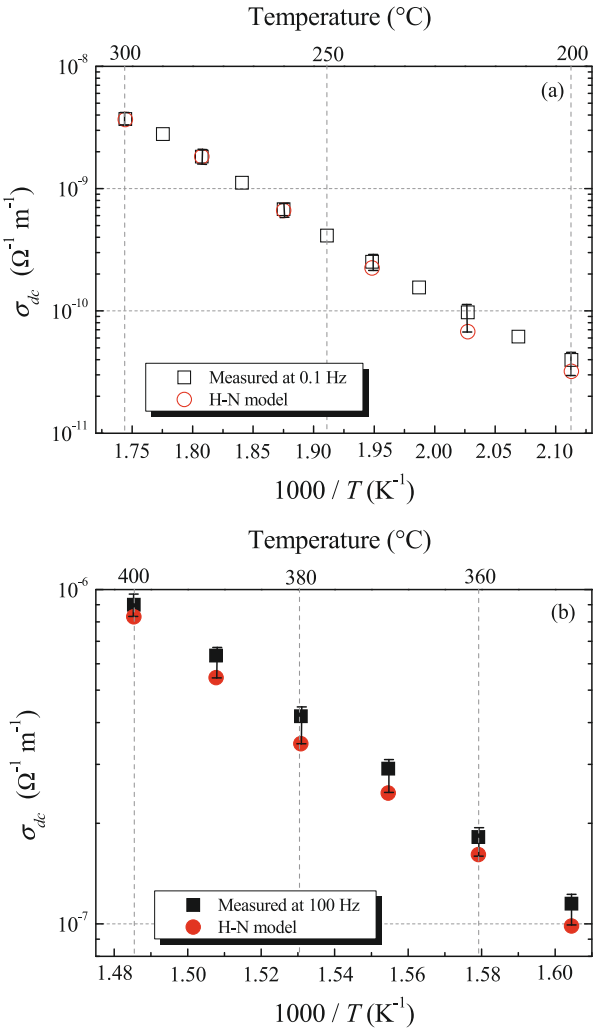

Fig. 6. (Color online) Comparison between measurements and modeling of the dc conductivity from (a) 200 to 300 °C at 0.1 Hz and from (b) 350 to 400 °C at 100 Hz.

According to the Coelho model describing analytically the dielectric behaviour of EP [28,54], a value of $\Delta\varepsilon'$ of 20 at LF/HT in MIMS are the consequence of the formation of a capacitance layer in the vicinity of each electrode with a Debye length (L_D, i.e. the space-charge layer thickness) of around 5% of the total insulating thickness. In the present PI MIMS case, L_D of the space-charge layer is evaluated around 100 nm for a 2 μm-thick PI film. Few data of L_D are available in the literature; however, let's note the results reported by Adamec and Calderwood on both epoxy resin and PI films [29]. In their work, they have evaluated (using another physico-analytic model) the space-charge thickness as close to 2.4% for a 500 μm-thick epoxy film in the range from 150 to 209 °C, and between 2.8 and 38% for a 25 μm-thick PI film from 111 to 200 °C. Our results appear so as consistent with these orders of magnitude.

The frequency dependence of the dielectric losses induced by the ρ- and ρ^*-relaxations may be obtained through the H−N model thanks to a multi-parameters numerical model. Unlike the α-relaxation, the magnitudes of the dielectric loss factor given by this model are nearly independent of the temperature, with values around 0.25 and 1 for the ρ- and ρ^*-relaxations, respectively. Using such a model is of course questionable, but the obtained values are however in close agreement with the $\tan\delta$ magnitude of the space-charge relaxation reported recently by Neagu et al. in PET and Lu et al. in Nylon 1010 between 110 and 200 °C [21,24].

Figure 5 presents the temperature dependence of the mean relaxation times τ_2 (ρ-relaxation) and τ_3 (ρ^*-relaxation). These two RPs exhibit an Arrhenius-like behavior following the equation:

$$\tau_i(T) = \tau_{0_i} \exp\left(\frac{E_{a_i}}{k_B T}\right), \qquad (5)$$

where E_a is the activation energy, τ_0 is the relaxation time at an infinite temperature (or the inverse of the vibration frequency of a charge carrier trapped in its site), k_B is the Boltzmann's constant ($k_B = 8.617 \times 10^{-5}$ eV K^{-1}), and T is the temperature. The ρ- and ρ^*-relaxations present activation energies respectively of 0.50 eV ± 0.01 eV and between 0.60 and 0.82 eV. Few articles report a qualitative and/or a quantitative description of EP usually observed around 150 °C up to 200 °C. Neagu et al. and Miyairi have shown in PET MIMS activation energies of 1 and 1.5 eV, respectively [19,21].

3.3 Discussion

The relevance of the proposed method for the σ_{dc} extraction is illustrated in Figure 6 which compares the values obtained from the plateau region of σ_{ac} measurements (i.e. extracted from Fig. 3, ignoring EP effect but taking into account an error bar) and those extracted from H−N fits

https://doi.org/10.1051/epjap/2009193 Published online by Cambridge University Press

(i.e. taking into account the EP influence). When the σ_{dc} and EP contribution occur in frequency ranges largely different, the measured and the calculated σ_{dc} values are almost identical (cf. Fig. 6a). On the contrary, Figure 6b demonstrates that the modeling becomes useful in the situations (i.e. temperature and frequency ranges) where the magnitude of the EP dielectric properties becomes no more negligible compared to the σ_{dc} response as may be seen at 100 Hz even above 350 °C in the BPDA/PDA case reported here. It is important to note the asymmetrical error distribution around the mean value of each experimental result which depends on both the frequency and the temperature: the largest value being obtained for the lowest temperature and/or the highest frequency.

Thanks to the proposed approach, the intrinsic dc bulk conductivity of dielectrics can be obtained accurately across a wide temperature range for relatively short time of measurements, i.e. a few seconds at a given temperature, thus leading to minimize the risk of premature ageing or degradation (oxidation, thermolysis) of the material during the measurements, which usually occur in most polymers in the high temperature range. This represents one of the greatest advantages of the DRS experiments coupled to the data processing method for investigating the electrical properties of insulating materials at high temperatures.

Finally, the H−N fitting procedure allows observing that the PI conductivity follows the Arrhenius law given by [12]:

$$\sigma_{dc}(T) = \sigma_0 \exp\left(-\frac{E_a}{k_B T}\right), \tag{6}$$

where σ_0 is the conductivity at an infinite temperature. The activation energy E_a of the conduction phenomenon obtained through the linear fit using equation (6) is around 0.55 eV. Moreover, PI films exhibit σ_{dc} values from 4×10^{-11} to 8×10^{-6} $\Omega^{-1}\,\mathrm{m}^{-1}$ for temperature between 200 and 400 °C, respectively. The values of σ_{dc} are in good agreement with values usually reported in the literature for other PI materials up to 250 °C, such as for polypyromellitimide films [55–57], and usually resulting from the conduction current experiments under static polarization. Such conductivity values indicate the semi-insulating character of the PI materials in such a wide temperature range close to the glass transition temperature. Indeed, it is supposed that both the thermal activation of the charge mobility lead to an increase of the ionic bulk conductivity (i.e. hopping charge transport), and to the decrease in the interface potential barriers with increasing temperature leading to an increase in the density of injected electrons (i.e. Schottky phenomenon).

4 Conclusion

The proposed analytic method for experimental data processing in MIM capacitor structures (MIMS) measured by dielectric relaxation spectroscopy (DRS) allows the quantification of the intrinsic dc bulk conductivity σ_{dc} in dielectrics without being impacted on by interface polarizations at LF/HT. Moreover, this method appears as a powerful alternative to much more time-consuming conduction current experiments. As an illustration of the method, a thermo-stable polyimide (PI) which is potentially interesting as an insulator in high temperature power electronics systems, has been characterized, being used as the inter-electrode dielectric material of MIMS. The method allowed the discrimination and quantification of the electrode polarization (EP) phenomenon occurring in MIMS at LF/HT, due to the build-up of a macroscopic space charge at the electrode interfaces. The dc bulk conductivity σ_{dc} in PI could then be quantified accurately in the high temperature range from 300 to 400 °C that was never reported before. It is shown that σ_{dc} of PI presents increasing values from 4×10^{-11} to 8×10^{-6} $\Omega^{-1}\,\mathrm{m}^{-1}$ for temperature between 200 and 400 °C. In the range from 200 to 250 °C, this material shows a similar behavior to those usually reported in the literature for polypyromellitimide films but obtained using the time consuming static polarization method. So, the proposed method appears as powerful and useful to study the dielectric material intrinsic properties at high temperature.

The authors are grateful to Mr. Benoît Schlegel for his technical contribution to this work.

References

1. C.P. Wong, *Polymers for Electronic and Photonic Applications* (Academic Press, London, 1993)
2. R. Kirschman, *High-Temperature Electronics* (IEEE Press, Piscataway, NJ, 1998), Part 8, p. 727
3. *Materials for High-Temperature Semiconductor Devices* (The National Academy Press, Washington, DC, 1995), Chap. 5, p. 51
4. R.W. Johnson, J. Williams, Mater. Sci. Forum **483–485**, 785 (2005)
5. S. Zelmat, M.L. Locatelli, T. Lebey, S. Diaham, Microelectron. Eng. **83**, 51 (2006)
6. J.R. Hanscomb, J.H. Calderwood, J. Phys. D: Appl. Phys. **6**, 1093 (1973)
7. E. Sacher, IEEE Trans. Electr. Insul. **EI–13**, 94 (1978)
8. E. Sacher, IEEE Trans. Electr. Insul. **EI–14**, 85 (1979)
9. G. Sawa, K. Iida, S. Nakamura, IEEE Trans. Electr. Insul. **EI–15**, 112 (1980)
10. M.H. Chohan, H. Mahmood, F. Shah, J. Mater. Sci. Lett. **14**, 552 (1995)
11. T.A. Ezquerra, J. Majszczyk, F.J. Baltà-Calleja, E. López-Cabarcos, K.H. Gardner, B.S. Hsiao, Phys. Rev. B **50**, 6023 (1994)
12. R. Casalini, D. Fioretto, A. Livi, M. Lucchesi, P.A. Rolla, Phys. Rev. B **56**, 3016 (1997)
13. R. Pelster, T. Kruse, H.G. Krauthäuser, G. Nimtz, P. Pissis, Phys. Rev. B **57**, 8763 (1998)
14. A. Bello, E. Laredo, M. Grimau, Phys. Rev. B **60**, 12764 (1999)
15. V. Bharti, Q.M. Zhang, Phys. Rev. B **63**, 184103 (2001)

https://doi.org/10.1051/epjap/2009193 Published online by Cambridge University Press

16. C. Svanberg, R. Bergman, P. Jacobsson, L. Börjesson, Phys. Rev. B **66**, 054304 (2002)
17. A. Dutta, T.P. Sinha, S. Shannigrahi, Phys. Rev. B **76**, 155113 (2007)
18. V. Adamec, J.H. Calderwood, J. Phys. D: Appl. Phys. **11**, 781 (1978)
19. K. Miyairi, J. Phys. D: Appl. Phys. **19**, 1973 (1986)
20. V. Adamec, J.H. Calderwood, IEEE Trans. Electr. Insul. **24**, 205 (1989)
21. E. Neagu, P. Pissis, L. Apekis, J.L. Gomez Ribelles, J. Phys. D: Appl. Phys. **30**, 1551 (1997)
22. E. Neagu, P. Pissis, L. Apekis, J. Appl. Phys. **87**, 2914 (2000)
23. H. Lu, X. Zhang, B. He, H. Zhang, J. Appl. Polym. Sci. **102**, 3590 (2006)
24. H. Lu, X. Zhang, H. Zhang, J. Appl. Phys. **100**, 054104 (2006)
25. K. Funke, C. Cramer, Curr. Opin. Solid State Mater. Sci. **2**, 483 (1997)
26. S. Diaham, M.L. Locatelli, T. Lebey, Appl. Phys. Lett. **91**, 122913 (2007)
27. F. Kremer, A. Schönhals, *Broadband Dielectric Spectroscopy* (Springer-Verlag, Berlin, Heidelberg, 2003)
28. R. Coelho, B. Aladenize, *Les Diélectriques* (Hermès, Paris, 1993)
29. V. Adamec, J.H. Calderwood, IEEE Trans. Electr. Insul. **24**, 205 (1989)
30. D.R. Day, T.J. Lewis, H.L. Lee, S.D. Senturia, J. Adhesion **18**, 73 (1985)
31. S.H. Liu, Phys. Rev. Lett. **55**, 529 (1985)
32. H.P. Maruska, J.G. Stevens, IEEE Trans. Electr. Insul. **23**, 197 (1988)
33. R. Díaz Calleja, J. Non-Cryst. Solids **172–174**, 1413 (1994)
34. V. Compañ, T.S. Sørensen, R. Diaz-Calleja, E. Riande, J. Appl. Phys. **79**, 403 (1996)
35. R.J. Klein, S. Zhang, S. Dou, B.H. Jones, R.H. Colby, J. Runt, J. Chem. Phys. **124**, 144903 (2006)
36. R. Bartnikas, R.M. Eichhorn, *Engineering Dielectrics, Vol. IIA – Electrical Properties of Solid Insulating Materials: Molecular Structure and Electrical Behavior* (ASTM-STP 783, Philadelphia, 1983)
37. A.K. Jonscher, Nature **267**, 673 (1977)
38. A.K. Jonscher, *Dielectric Relaxation in Solids* (Chelsea Dielectrics Press, London, 1983)
39. A.K. Jonscher, J. Phys. D: Appl. Phys. **32**, R57 (1999)
40. T. Tanaka, S. Hirabayashi, K. Shibayama, J. Appl. Phys. **49**, 784 (1978)
41. A.A. Alagiriswamy, K.S. Narayan, G.R. Govinda Raju, J. Phys. D: Appl. Phys. **35**, 2850 (2002)
42. M. Garg, J.K. Quamara, Nucl. Instrum. Meth. B **246**, 355 (2006)
43. V. Adamec, Polymer **15**, 496 (1974)
44. K. Miyairi, J. Phys. D: Appl. Phys. **19**, 1973 (1986)
45. M. Pollak, T.H. Geballe, Phys. Rev. **122**, 1742 (1961)
46. S. Havriliak, S. Negami, J. Polym. Sci. C **14**, 99 (1966)
47. S. Havriliak, S. Negami, Polymer **8**, 161 (1967)
48. K.S. Cole, R.H. Cole, J. Chem. Phys. **9**, 341 (1941)
49. D.W. Davidson, R.H. Cole, J. Chem. Phys. **19**, 1484 (1951)
50. R. Casalini, A. Livi, P.A. Rolla, G. Levita, D. Fioretto, Phys. Rev. B **53**, 564 (1996)
51. I.M. Kalogeras, M. Roussos, A. Vassilikou-Dova, A. Spanoudaki, P. Pissis, Y.V. Savelyev, V.I. Shtompel, L.P. Robota, Eur. Phys. J. E **18**, 467 (2005)
52. K.U. Kirst, F. Kremer, V.M. Litvinov, Macromolecules **26**, 975 (1993)
53. C. Hakme, I. Stevenson, L. David, G. Boiteux, G. Seytre, A. Schönhals, J. Non-Crystal. Solids **351**, 2742 (2005)
54. R. Coelho, Rev. Phys. Appl. **18**, 137 (1983)
55. V. Adamec, J.H. Calderwood, J. Phys. D: Appl. Phys. **8**, 551 (1975)
56. G. Sawa, S. Nakamura, K. Iida, M. Ieda, Jpn J. Appl. Phys. **19**, 453 (1980)
57. G.M. Sessler, B. Hahn, D.Y. Yoon, J. Appl. Phys. **60**, 318 (1986)

https://doi.org/10.1051/epjap/2009193 Published online by Cambridge University Press